

Poster: Acoustic Backscatter Communication In Realistic Metal Structures

Peter Oppermann
peter.oppermann@tuhh.de
Hamburg University of Technology
Hamburg, Germany

Bernd-Christian Renner
christian.renner@tuhh.de
Hamburg University of Technology
Hamburg, Germany

ABSTRACT

This study demonstrates the feasibility of acoustic backscatter communication in complex metal structures, extending previous work that focused on simple, isolated metal specimens. Real-world measurements examine one-way channel gains and backscatter signal strengths across various structural elements, including weld and screw connections. Results demonstrate successful communication over a 3-element, 13-meter channel with significant attenuation.

CCS CONCEPTS

• **Hardware** → **Wireless devices**; • **Computer systems organization** → *Sensors and actuators*.

KEYWORDS

acoustic communication, passive communication, metal

1 INTRODUCTION

Communication in metal structures enables numerous applications in structural health monitoring for industrial and civil infrastructure [4]. Among different techniques, passive backscatter tags have been shown to extend battery life or enable batteryless sensors [1, 2]. However, existing studies (e.g. [2]) demonstrated feasibility in small and simple specimens, such as isolated, flat metal bars. This poster shows preliminary results from our ongoing effort to extend backscatter communication to larger structures, consisting of multiple structural elements embedded within buildings and including weld and screw joints. Therefore, we measure the one-way channel gain and demonstrate that our existing prototypes already enable backscatter communication through a complex structure with two weld connections over more than 13 m.

2 METHODS

A monostatic backscatter system consists of a reader and a tag. The tag communicates passively by reflecting incoming acoustic waves at its transducer, while the reader actively generates the carrier and receives the backscattered signal. We employ existing hardware (see Fig. 1) for reader and tag presented in [3], featuring 28 V_{pp} amplitude carrier waves and analog filtering and demodulation of the backscattered signal. Finally, we use a TiePie HS-5 oscilloscope to sample the resulting signals.

During experiments, we attach off-the-shelf piezoelectric disk transducers from PICeramics to the structure's bare metal surfaces using epoxy resin. Since the frequency range for most-efficient lamb-wave generation depends on material thickness, we adapt transducers to the structural element, i.e., we choose transducers with 10 mm diameter (resonance around 200 kHz) for thin metal structures, and with 25 mm diameter (resonance around 80 kHz) for

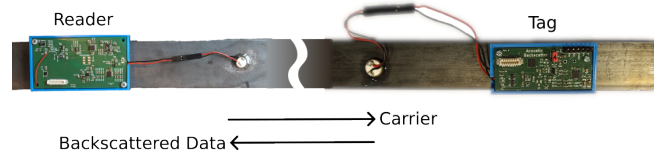


Figure 1: The employed hardware prototypes.

thicker ones. To assess the feasibility of communication through larger structures, we investigate two metrics: First, we measure the forward channel gain between two transducers, and, second, the full two-way backscatter channel.

Channel Gain

To estimate the channel gains between two transducers, the reader generates a linear chirp within 10–500 kHz, while the oscilloscope records the transmitted and received signals $x(t)$ and $y(t)$ at both transducers. The frequency response $H(f)$ is then given as

$$H(f) = \frac{Y(f)}{X(f)}, \quad (1)$$

where $X(f)$ and $Y(f)$ are the Fourier transforms of $x(t)$ and $y(t)$. The frequency-dependent channel gain is the magnitude of $H(f)$.

Backscatter Signal Strength

To further determine the strength of the backscattered signal, the reader generates a continuous sine carrier. The battery-powered tag, on the other hand, modulates the incoming carrier with an 8 kHz square wave, encoding a 13-symbol Barker sequence with 0.5 ms symbol duration (total signal duration 6.5 ms). The signal repeats every 100 ms. The RX signal's average amplitude σ_s is derived from the baseband signal $b(t)$ correlated with the Barker sequence $B(t)$ and normalized with the sequence's magnitude, i. e. ,

$$\sigma_s^2 = \frac{b(t) * B(-t)}{\int B^2(t) dt}. \quad (2)$$

Since metal channels are usually highly frequency-selective, σ_s depends heavily on the selected carrier frequency.

3 RESULTS

We investigated three complex structures (see Fig. 2). First, a 6 m long beam with a square profile (SP), including signal propagation around corners. Second, an arch composed of three individual SP beams, joined by two weld connections, with total propagation distance between transducers of 13 m. Lastly, we investigated a 10 mm strong H-beam, including a channel through a screw connection. To match structural resonance frequencies, we used the smaller

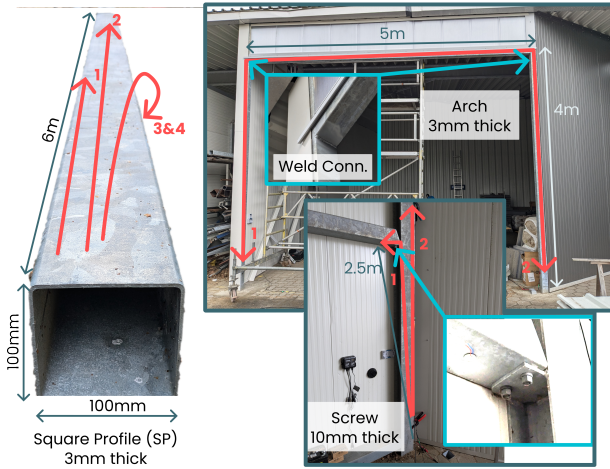


Figure 2: Three different structural elements were investigated, including corners and weld and screw connections.

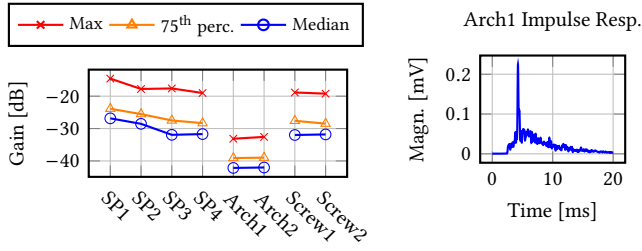


Figure 3: Maximum (at best carrier), median, and 75th percentile gain in different channels (left) and impulse response of 13m long channel Arch1 (right).

transducers with higher resonance frequency for the former two structures, and larger transducers for the latter.

One-way Channel Gain. To compare the strongly frequency-dependent gain between different channels, Fig. 3 (left) shows the distribution of the gain’s magnitude within the transducer’s resonance bands (200–240 kHz for SP and Arch, 90–120 kHz for Screw). All channels show a similar 10–12 dB gain difference between best (Max) and median frequency, emphasizing the potential of frequency calibration to maximize channel gain. In the SP structure, optimal and median gains decrease only slightly with longer distances, and signal propagation around corners only moderately impacts gain. Surprisingly, even through the screw connection, the gains are comparable to the isolated SP profile element. Finally, gains through the arch are significantly lower, at maximum close to -30 dB, which is expected due to the much longer distance and multiple weld connections. The arches’ channel impulse response in Fig. 3 (right) also shows a large delay spread of more than 15 ms, complicating communication.

Backscatter Signal Detection. Fig. 4 (left) shows the backscatter signal strength distributions σ_s compared to the noise standard deviation in selected backscatter channels¹. The SP channels achieve

¹Unfortunately, we could not evaluate the backscatter signal in the Screw channels, because the reader’s frequency range was incompatible with the lower resonance

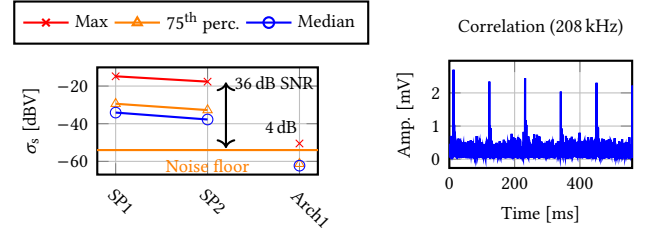


Figure 4: Backscattered signal strength compared to the noise standard deviation (left), and correlation with transmitted signal at best frequency in Arch1.

a maximum SNR above 36 dB, more than sufficient for communication. In the Arch channels, the best frequencies have a 32 dB lower SNR—still feasible for communication, but likely requiring slower, more robust schemes. Fig. 4 (right) shows the correlation’s magnitude with clearly distinctive peaks for every transmitted sequence (repeated every 100 ms).

4 DISCUSSION AND CONCLUSION

The study investigated the channel gains and backscatter signal strengths in complex metal structures. We demonstrated that communication with our existing reader and tag prototypes is feasible even over a 13-meter channel comprised of three distinct elements, joined by two weld connections. Furthermore, forward channel gains indicate good performance even through screw connections.

While the received signals are weaker in composite channels, we emphasize that 1) the reader prototype currently uses only about 100 mW signal power—ten times less than a commercial RFID reader, and more than 1000 times less than state-of-the-art underwater backscatter systems [1], and, 2) the used hardware is a research prototype that can likely be optimized to achieve higher SNRs. Hence, there is large potential for further range extension with increased signal power and lower-noise hardware.

5 ACKNOWLEDGMENTS

The authors would like to thank Stefan Gehrman and Gehrman Baugesellschaft m.b.H. for providing access to a storage depot to carry out the measurements in this work.

REFERENCES

- [1] S. S. Afzal, W. Akbar, O. Rodriguez, M. Doumet, U. Ha, R. Ghaffarivardavagh, and F. Adib. Battery-free wireless imaging of underwater environments. *Nature Communications*, 13(1), 2022.
- [2] P. Oppermann and B.-C. Renner. Equalization for High-Bitrate Acoustic Backscatter Communication in Metals. In *EWSN’22: Proc. of the 2022 International Conference on Embedded Wireless Systems and Networks*, 2022.
- [3] P. Oppermann and B.-C. Renner. Acoustic backscatter communication and power transfer for batteryless wireless sensors. *Sensors*, 23(7), 2023. DOI: 10.3390/s23073617.
- [4] Y. Sun, Y. Xu, W. Li, Q. Li, X. Ding, and W. Huang. A lamb waves based ultrasonic system for the simultaneous data communication, defect inspection, and power transmission. *IEEE Tans. on Ultrasonics, Ferroelectrics, and Frequency Control*, 68(10), 2021.

transducers. However, the strong channel gains indicate backscatter performance similar to SP channels.